The failure process of the filled loess slope triggered by groundwater using a flume test

Jianqi Zhuang[1], YI Zhu[2], Yong Zhao[1], Yanqiu Leng[1], Xinghua Zhu[1], Weiliang Huang[1], and Jianbing Peng[1]

[1]Chang'an University
[2]Changan University

May 15, 2020

Abstract

Gully Stabilization and Highland Protection (GSHP) techniques are useful in preventing gully erosion and have been widely utilized in the Loess Plateau. Rolling backfill is used to fill ditches in remolded loess, which is an important part of gully stabilization and highland protection, but destroys the original loess structure and changes the circulation of groundwater and surface water leading to a rise in groundwater. Groundwater rising is an important factor for filled loess slope instability and can induce landslides. A test device was designed to study the process of water infiltration into the filled project and the failure process of the filled loess slope due to groundwater rising. First, the groundwater was uniformly infiltrated with water, then preferential seepage with the deformation and cracks appeared in the slope. The pore-water pressure response to the groundwater infiltration and the pore-water pressure in the front of the slope body sharply increased, especially near the sliding surface, while the pore-water pressure at the back of the slope sharply decreased during slope failure. The failure process of the experimental slope can be divided into three stages: settlement deformation, collapse deformation, and slope toe slide-flow or regressive failure. In the first and second stages, the deformation is vertical displacement as slope settlement, and the third stage deformation is mainly horizontal displacement in the direction of the free surface of the slope body. The filled slope failure is due to groundwater infiltration with suffusion erosion, saturated softening, and infiltration dynamics.

KEYWORDS:

Loess-filled slope; Groundwater rising; Failure process; GSHP; Loess Plateau

1. Introduction

Loess is mainly distributed in semi-arid and arid areas and forms three characteristic types of geomorphic structures: loess tableland, loess ridge, and loess dome (Liu, 1985). The terrain of loess tableland is flat and is the most valuable land resource suitable for farming and living in the Loess Plateau (Liu, 1985; Derbyshire, 2001). Among them, Dongzhiyuan (yuan means tableland in Chinese) in Qingyang, Gansu Province, has the thickest deposited loess and the biggest area loess tableland of the world, known as "the first loess tableland in the world." The gully erosion caused by urban construction and agricultural development has become increasingly serious (Derbyshire et al., 2000; Wu and Cheng, 2005). With the frequent occurrence of extreme climate in northwest China, and the irrigation projects on the tableland, gullies around the Loess Tableland are constantly eroding to the center of the loess tableland and separating it (Lu et al., 2011; Qi et al., 2017). In recent years, with urban development and agricultural activities, both the gully erosion and soil erosion in the Dongzhiyuan tableland are becoming increasingly serious. They tend to extend towards the center of the highland and causes the highland to become fragmented (Figure 1). Note that the east-west width of this highland has decreased from 32.0 km in the Tang Dynasty to 17.5 km currently, while the east-west width at its narrowest is only 50 m (Shi, 1987; Chen et al., 2009). In such a circumstance, the GSHP project has been undertaken in the Loess Plateau. For example, Qingyang in Gansu Province has carried out "GSHP" to solve the problem of retrogressive erosion in the loess tableland area, and has carried out the ditch head landfill work on 14,035 gullies in the Dongzhiyuan tableland. According to the data from the Qingyang Water and Soil Conservation Administration, the area of soil erosion in the Dongzhiyuan tableland has accounted for more than 96% of the total area, where approximately 66 million tons of silt has been transported to the Yellow River each year; and in some regions, the highland was already collapsed (Xifeng Soil and water conservation Observation station of Yellow River Conservancy Commission of the Ministry of Water Resources, 2005). In 2017, Qingyang completed the gully protection project with an investment of 152 million yuan. At the same time, the Management Committee of the Middle and Upper Reaches of the Yellow River has implemented plans to carry out GSHP for erosive gullies threatening the Loess Plateau over the next 20 years.

Figure 1 Gully erosion in the Dongzhiyuan tableland, where the highland is fragmented

However, according to our field investigation, it was found that all projects suffered erosion damage within one year (Figure 2). In the GSHP project, the remodeled loess ditch was filled with rolling backfill, which destroyed the original loess structure, and changes the circulation of groundwater and surface water, leading to a rise in groundwater (Yin et al., 2016; Zhao et al., 2018; Wang et al., 2018). It is known that remolded loess is more likely to collapse and lose its strength under water action. According to experiments, even the dry density of remolded loess is more than that of undisturbed loess and the strength of remolded loess will sharply decrease and collapse after water infiltration occurs (Yang et al., 2003; Wang et al., 2018). The existing gully head is often the discharge outlet of the groundwater in the tableland area. Once filled, it will lead to a large amount of groundwater converging on the filled loess, which will soften the filled loess and lead to filled loess instability. For example, the remolded loess filled the groundwater channel, which resulted in groundwater rising and infiltrating the filled loess, then a landslide occurred in 2011 shortly after the project and buried the county square and affected the deformation of residential buildings in the Dongxiang County of Gansu Province (Zhuang and Peng 2014). A gully was filled with the remolded soil in Shichuan Town, Lanzhou, and the filled remolded soil failure in 2015 was due to the groundwater rising and water infiltration, and then the failure changed to debris flow forming the landslide-mudflow chain disaster event (Zhang et al., 2019). The erosion phenomenon and groundwater rising have already appeared in the Gully Stabilization and Highland Protection project (Singh et al., 2010; Jin et al., 2019). The Gully Stabilization and Highland Protection project will face failure risks due to erosion and rising groundwater. Nature has published a comment article and called for the implementation of relevant research projects as soon as possible to deal with the various new problems brought about by major engineering construction (Li et al., 2014).

Figure 2 The Gully Stabilization and Highland Protection projects damaged by erosion

Loess is a special soil that is sensitive to water and prone to failure in excess water situations (Zhuang et al., 2017). It is very important to carry out studies on the characteristics of groundwater change in loess areas, especially the characteristics of groundwater change in loess-filled areas (Li et al., 2014). Most literature has reported groundwater changes in filled projects (Singh et al., 2010; Jin et al., 2019), simulation of the groundwater reconstruction process in filled projects (Langevin and Guo, 2014; Li et al., 2017), and monitoring the groundwater reconstruction path in filled projects (Yu et al., 2014; Zhang et al., 2017). Filled engineering construction has changed the original topography and geological structure, which will block the channels and spring holes, thus changing the original groundwater seepage path. Meanwhile, the infiltration rate of compacted filled soil is lower than that of undisturbed soil, which makes the groundwater infiltrate into the filled soil, resulting in rising groundwater in the filled project, and then the filled projects will have deformation and instability. Yin et al. (2016) predicted groundwater changes in highly filled projects using numerical simulation and showed that the groundwater level will likely rise in filled project bodies over the next 50 years. Groundwater plays an important role in the filled project deformation and failure due to rising groundwater and infiltration into the filled project body (Yin., 2016; Wang et al., 2018). Some scholars focus on the catastrophic effects of groundwater rising caused by filled engineering, such as pore-water pressure increase caused by groundwater (Yin et al., 2016; Jin et al., 2019), the sensitivity of the filled body to vibration and the vibration liquefaction (Wang et al., 2018), and large deformation due to rising groundwater in a filled body (Song et al., 2008), which will have an important impact on the stability of the filled project. The large-scale, filled projects in the Loess Plateau, such as Gully Stabilization and Highland Protection, are likely to generate a catastrophic landslide event similar to the Guangming landslide that occurred in Shenzhen on Dec. 20, 2015 due to rising groundwater (Yin et al., 2016).

Loess has special characteristics of macro-pores, vertical joints, loose texture, and water sensitivity, especially remolded loess, which makes it prone to erosion (Derbyshire, 2000; Dijkstra, 1995; Zhang et al., 2009; Zhuang et al., 2017). Rising groundwater is one of the most important factors for filled slope instability and can induce a series of geohazards such as collapse, landslide, and debris flow. In Qingyang City, Gansu Province, note that although the implementation of the Gully Stabilization and Highland Protection can effectively alleviate gully erosion and soil erosion, the groundwater rising can cause failure due to the filled projects blocking the groundwater discharge and should be given more attention. To study the stability and failure mode of the filled project caused by the groundwater rising, a test device was designed to study the process of water infiltration into the filled project and the failure mode of the filled project due to groundwater rising.

2. Setting area

The Dongzhiyuan loess tableland with the north-south strike located in the eastern part of the Gansu Province is called the 'biggest loess plateau'. The loess of the Dongzhiyuan tableland is almost 300 m in depth. The upper layer is mainly composed of Malan loess, about 20-40 m thick, deposited in the late Pleistocene period (Q3). The geomorphology of the Dongzhiyuan tableland belongs to the typical loess plateau tableland-gully, which has characteristics of the tableland surface that are flat and the gully is crisscross around. Since 2000, the back erosion of gullies around the Dongzhiyuan tableland has been intensified because of population growth and increased human activities. The gully and soil erosion in the Dongzhiyuan tableland are becoming increasingly serious and extend towards the center of the highland, which causes the highland to be fragmented (Figure 1). Geohazards, such as landslides and collapses, occur frequently. Since the Tang Dynasty, the eroded area of the tableland has reached more than 599.6 km^2, with an average annual loss of about 0.46 km^2. According to the investigations, the original Dongzhiyuan tableland was divided into 11 pieces in the last 1300 years, with the largest at 946.25 km^2 and the smallest at 0.39 km^2(Shi, 1987; Chen et al., 2009).

So, Qingyang in Gansu Province has carried out the major project of "GSHP" to solve the problem of retrogressive erosion in the loess tableland area, and has carried out ditch head landfill work on 14,035 gullies in the Dongzhiyuan tableland. The Dongzhiyuan tableland is the most common location for GSHP filled soil failure research.

In this paper, the Huoxiang gully, which has been carried out by the GSHP in 2017 and finished in 2018 is taken as a case study. Huoxiang gully, located in the east of the Dongzhiyuan tableland, belongs to the Malian River basin. The gully erosion and the soil erosion in the Huoxiang gully have become increasingly serious over the past 15 years due to water drainage from the city. The gully back erosion is more than 30 m with an average annual head back erosion of more than 2 m since 2004, and the cut erosion has increased to 40 m. The continuous head back erosion poses a great threat to the local people. So, the GSHP project was carried out and the head of the gully was filled in 2017. According to the DEM (tandem with 5 m resolution) pre-filled and the design of the filled project, the maximum landfill depth is 80 m and the width is 300 m (Figure 3).

Figure 3 The GSHP in the Huoxiang gully

From the topographic map and field investigation, the altitude of the head of the Huoxiang gully is lower than that of the Dongzhiyuan tableland surface and the head of the gully is the groundwater outlet of the tableland before landfilling. The GSHP changes the circulation of groundwater and surface water, leading to a rise in groundwater. The groundwater infiltrates into the filled project and softens the filled loess, resulting in filled project failure.

3. Material and method

3.1 Material

The soil used in the experiments was loess from the Huoxiang gully with a mean particle size (D50) of 0.57 mm containing more than 17.3% clay ([?]0.005 mm). The experimental slope was placed in layers and compacted to the specified density (dry density (1.52 g/cm^3)) according to a standard of 5 cm for each layer. The experimental slope was constructed with a gradient of 40°. The initial moisture content was determined by collecting and drying the soil samples prior to the experimental runs. In the experiment, the initial moisture content of the soil was measured to be about 12.20%. The strength of the specimen under different confining pressures was tested by an unsaturated soil stress-strain controlled triaxial apparatus. The physical characters of the soil in the test are similar to the filled project (Table 1).

Table 1 The basic physical property parameters of the loess

	Natural water content	Natural dry density	Plastic limit	Liquid Limit	Plasticity index	Particle size(%)	Particle size(%)	Particle size(%)
	w/(%)	ρ/(g·cm^{-3})	W_P /(%)	W_L/(%)	I_p/(%)	>0.075 mm	0.005-0.075 mm	<0.005
Loess sample	12.2%	1.70	17.3	30.5	13.2	8.58	72.67	18.75

3.2 Method

The device consists of three parts: slope flume, rainfall operator, and data acquisition system. The slope flume is a three-dimensional experimental loess slope constructed in a 2 m × 0.6 m × 1.2 m (length × width × height) box with glass sidewalls and a metal frame (Figure 4).

The data acquisition system is composed by nine EC-5 volumetric water content sensors, each with an accuracy of ±2%, nine MKM pore-water pressure sensors and a displacement sensor with an accuracy of ±0.1 mm, that were installed at specific depths as the slope was constructed. The sensors were each connected to two Em50 data loggers. The sensors were calibrated before each experiment.

Surface deformation was monitored using a 3D laser scanner with 1-mm precision and high-resolution topographic data was obtained by repeatedly scanning the experimental slope surface every 30 min during each experiment. Polyworks software were used to process the data and quantitatively describe slope deformation and failure characteristics.

To accurately simulate the rising groundwater and infiltration into the filled project, the groundwater was recharged through the concentrated channel by locating the drainage plate and temporary water tank at the rear of the experimental model. The water in the temporary water tank was kept at a constant height of 40 cm. The drainage plate was set in five rows spaced at 20 mm, whereas the columns were spaced at intervals of 20 mm. The diameter of the drainage holes was 2.0 mm to ensure that the groundwater was able to infiltrate into the slope evenly.

Figure 4 Schematic drawing of the groundwater uplift test flume setup

4. Results

4.1 The groundwater infiltration process

The groundwater diffuses towards the surface of the slope from the back of the slope in the initial stages. With rising groundwater, the height of water entering the slope was consistent with the rising height of groundwater without forming preferential seepage. In this process, the water softens the soil and causes deformation of the slope with infiltration into the slope. The cracks appear in the slope due to deformation resulting in the groundwater forming preferential seepage along the cracks and entering the soil quickly. Figure 5 shows the change in water content of the slope vs time at different positions. The water content at the back of the experimental slope increases immediately with increasing groundwater levels, and the water content at the front of the experimental slope relatively increase later. Meanwhile, the upper water content increases slowly due to the groundwater increasing from bottom to top. Then the groundwater continues to infiltrate from the back of the slope and seeps out from the toe of the slope. The water transfer path formed, and the slope failure occurred at 316 mins. The water content near the slope toe at 20 cm responds to the failure and increases quickly, which shows that the slip surface is near this area. The hydrostatic pressure near the sliding surface increases during failure, resulting in increasing water content, which indicates that the shear contraction appears in the sliding surface.

Figure 5 Change in water content of the slope vs. time at different positions (a: position at back of the slope; b: position at front of the slope)

During the test, although the groundwater seeps out from the middle of the slope surface and then spreads to the slope toe, the slope is still stable even if the middle of the slope is saturated. Until the groundwater seeps out from the slope toe, the slope begins to fail via the retrogressive sliding process (Figure 6). This phenomenon shows that the slope would not fail due to saturated soil in any area of the slope and will fail due to the key part of the slope saturation. The stress distribution of the slope is uneven and concentrated at the slope toe, resulting in this area being prone to failure. The slope toe fails first and makes the upper part fail resulting in a regressive landslide. This phenomenon is consistent with that observed at Heifangtai, most of the landslide at Heifangtai failure until the seepage out from the slope toe and the slope toe failure first and then makes the upper part failure resulting in forming regressive landslide. The results show that the key blocks have great influence on the stability of the slope.

Figure 6 Water infiltration process

4.2 Pore-water pressure changes

The experimental slope body also responds to the groundwater rising including the increase of water content, pore-water pressure and deformation when groundwater infiltrates into the experimental slope.

Groundwater infiltrates from the back to the front of the experimental slope resulting in pore-water pressure at the back of the slope increasing sharply with the increase of groundwater level. Meanwhile, the pore-water pressure at the front of the experimental slope does not fluctuate because the water is not infiltrating into this area (Figure 7). The pore-water pressure of the soil at different heights at the back of the slope responds to the groundwater rising differently. The pore-water pressure of the soil below the height of the groundwater level increases immediately and sharply as the groundwater rises and infiltrates, while the pore-water pressure of the soil above the height of the groundwater level increases gradually with a time lag. The experimental slope settlement deformation due to groundwater infiltration results in cracks on the slope.

Figure 7 Change in pore-water pressure of slope vs time at different positions (a: position at back of the slope; b: position at front of the slope)

The groundwater infiltrates to the front of the slope resulting in the pore-water pressure of the soil in this area starting to rise with continuous groundwater infiltration. The groundwater infiltrates into the front of the slope after about 190 mins. The pore-water pressure of the soil at the bottom of the experimental slope gradually increases with groundwater infiltration, and the pore-water pressure of the upper soil does not change.

The groundwater seeps out from the experimental slope toe due to continuous infiltration of groundwater, and the soil at the toe of the slope is saturated. The pore-water pressure sharply increases resulting in the effective stress of the soil decreasing, and the slide-flow occurs from the toe of the slope which results in experimental slope failure of overall instability as a regressive landslide process. The pore-water pressure in the front of the slope body sharply increases, especially the pore-water pressure near the sliding surface, which substantially increases. However, the change in pore-water pressure at the back of the slope sharply decreases in the failure process, while the pore-water pressure at the front of the slope increases during the failure process (Figure 7). Both result in slope failure, but the pore-water pressure shows a difference, which indicates that the slope toe shows shear contraction characteristics resulting in a sharp increase in pore-water pressure, while the back of the slope shows a state of tensional stress, resulting in sharply decreasing pore-water pressure.

4.3 The failure processes

During the test, the deformation process of the experimental slope can be divided into three stages as follows:

(1) Settlement deformation. The groundwater gradually infiltrates into the experimental slope with rising groundwater. The water content of the soil increases due to water infiltration, resulting in decreasing loess strength. Meanwhile, the loess with the water infiltration occurs suffusion erosion which cause loess collapsibility and volume decrease resulting in settlement. Settlement cracks at different depths were induced due to the differential settlement and suffusion erosion in the slope body, and the settlement cracks gradually extend in length and width with the continuous infiltration of groundwater (Figure 8a).

(2) Collapse deformation. The settlement cracks continue to expand and form a curtain with cracks due to continuing suffusion erosion, and then the soil of the upper layer collapses due to gravity. The internal soil collapse of the slope makes the surface of the slope deform, which induces cracks on the surface of the slope. The cracks extend and connect to each other, and then preferential seepage routes are formed in the slope which become potential sliding surfaces (Figure 8b).

(3) The slope toe slide-flow and failure. The groundwater infiltrates to the slope toe and seeps out. The soil at the toe of the slope is saturated, and the effective stress decreases resulting in sliding and flowing. Then the slope toe forms a free surface resulting in the upper part of the slope failing after losing the support of the lower soil mass, and then the slope failure is a regressive landslide (Figure 8c).

In the first and second stages, the deformation is vertical displacement of slope settlement, and in the third stage, the deformation is mainly horizontal displacement with the direction to the free surface of the slope body.

Figure 8 Deformation process of the experimental slope

5. Discussion

The land-filled gully by the Gully Stabilization and Highland Protection is usually the discharge outlet of the groundwater and urban sewage outfall. The seepage of the groundwater enters the filled slope from the back, which is different from the mechanism of the rising groundwater in the reservoir or the rising groundwater caused by irrigation. In this process, groundwater infiltrates into the filled slope and produces a variety of effects on the slope, including suffusion erosion, saturated liquefaction, and infiltration dynamics.

5.1 Suffusion erosion

The process of suffusion erosion is different from that of surface erosion (Kovacs, 1981; Kenney and Lau, 1985; Chapuis, 1992; Bendahmane et al., 2008). Lots of researchers describe suffusion erosion as the "redistribution or transport of small particles of fine grains within the layer. . . " according to the physical phenomenon (Kovacs, 1981; Chapuis, 1992; Moffat and Fannin, 2006; Zhuang et al., 2015b). Furthermore, particle migration yields a reduction in total volume and a potential for collapse of the soil matrix and soil strength (Vallejo, 2001; Mao, 2005; Richards and Reddy, 2007; Chang and Zhang, 2013). Scholtès et al. (2010) noticed that suffusion may trigger the soil state to change from "dense" (below the critical state line) to "loose" (above the critical state line) via fine grain extraction. Additionally, local mechanical and hydraulic variations due to fine particle migration influence the stability of the soil slope.

To perform suffusion erosion tests of the remolded loess sample, a suffusion permeameter was used to simulate the water infiltrated into the loess. It is constituted by a cylindrical seepage cell made of plexiglass to allow visual observation of particle migration, the water tank, fines collector, and water supply tank. The cell has an inner diameter of 70 mm and height of 140 mm and can allow for (difference in hydrostatic head-driven) water permeation and retain a reservoir of water above the loading cap and sample. The loading cap was filled with a 2 mm glass ball to promote the water to enter the loess evenly. The cylindrical seepage cell was placed with the transparent waterproof adhesive to the side wall of the sample, which was used to make the sample and the cell close without sidewall seepage. The remolded loess soil from the filled slope with the same character of the experimental slope was placed into the cylindrical seepage cell layer by layer. The Perspex cap has a number of small (2 mm) holes and was placed between the sample and bottom of the cell to improve the water flow and fine particles from the sample to the fine particle and water collection box (Figure 9).

Figure 9 Testing apparatus to simulate internal erosion under water infiltration

During the 30 day infiltration process, the cumulative amount of water seepage out was 19.369 L and the total amount of soil particles carried out by the seepage water was 0.52 g. The clay content accounts for 19.54% ($d < 0.005$ mm), the silt content accounts for 74.96% ($0.075 > d > 0.005$ mm), and the sand content accounts for 5.47% (0.075-2 mm) of the fine particles carried out by the seepage water (Figure 10).

Figure 10 Particle size distribution of the original and carried out sample

It can be found that the fine particles migrated out by suffusion were mainly clay and silt particles. The migration of fine particles changed the soil skeleton and increased the porosity and infiltration rate of the sample. According to soil tested after oven drying of the soil sample column, the dry density of the soil sample column decreased from 1.44 g/cm^3 to 1.382 g/cm^3, and the void ratio increased from 0.875 to 0.954 after 30 days of water infiltration.

Loss of particles due to internal erosion can reduce the soil volume and lead to the potential collapse or settlement of the soil skeleton (Crosta and di Prisco, 1999; Moffat et al., 2011; Chang and Zhang, 2013; Fan et al., 2017). This phenomenon of infiltration settlement is very common in Heifangtai (Zhang and Wang, 2018; Shi et al., 2019).

With infiltration, the soil sample column shows obvious settlement in the vertical direction. After 80 minutes, the water infiltrates from the top to the bottom of the soil sample, and begins to flow out from the bottom of the soil sample. In 20 h, the number of fine particles that move out with the water is very few, and with the infiltration, the water seepage out increases significantly, and the fine particles carried out have increased. This shows that the fine particles can migrate with the water, resulting in a changing infiltration rate of the soil sample and increasing hydraulic conductivity. In the first two days, the volume of the soil sample column did not change and began to appear to settle after 48 h with continued infiltration. After 58 h, the settlement of the soil sample column was up to 1 cm. After 15 days, the settlement was up to 2 cm, and then the settlement was increased with the water infiltration, the settlement was up to 3 cm after 23 days. After 30 days, the settlement was 3.3 cm and the settlement ratio reached 16.5%.

So, the suffusion erosion will occur with groundwater infiltrating into the filled slope and cause the migration of fine particles. The migration of fine particles will change the structure of the filled slope resulting in a collapsed settlement, which is similar to the experimental phenomenon.

5.2 Saturation softening

Groundwater will increase the water content of loess, especially the long-term effects of groundwater, which will saturate the soil. Since loess is highly sensitive to water, the strength of the loess will sharply decrease with increasing water content (Zhuang et al., 2015a; Peng et al., 2018).

The isotropically consolidated undrained triaxial test (ICU) is a common procedure used to study soil strength at different axial stress and shear levels. For this study, remolded loess sample, with an approximate volume of 30 cm × 30 cm × 30 cm, were retrieved from a filled slope in Qingyang. A subsample of 100 mm height and 50 mm diameter was extracted for subsequent tests. The shear stress is defined by σ1' (the maximum effective principal stress)-σ3' (the minimum effective principal stress), and the effective stress path is defined by (σ1'+2×σ3')/3. The samples used in the triaxial test were wetted to saturation with distilled water assisted by CO_2 until a pore pressure coefficient (*BD*) (Sassa, 1985) of 95% was exceeded. The samples were then compressed under undrained conditions following the strain-controlled method. The confining pressures were 100, 200, and 300 kPa, and the shear velocity was fixed at 0.07 mm/min.

Figure 11 shows pore-water pressure graphed against axial strain. At all three normal stress levels, the pore pressures generated attained values up to the normal stress when the axial strain reached 15%. After this, steady state resistance was observed. The path of effective stress indicated that the effective stress decreased with shear strain, and the final points were less than 40 kPa (Figure 11b), indicating that cohesive strength was completely lost. This enabled liquefaction in the presence of saturation shearing.

The strength of loess decreases, especially while the strength of loess at the slope toe decreases, the slope fails in sequence of slope toe sliding. Meanwhile, the phenomenon of shear contraction can be observed by the triaxial test, which is also the reason for the sharp increase of pore-water pressure during the sliding slope. The sharp increase in pore-water pressure leads to further decreases in loess strength, which promotes slope failure.

Figure 11 ICU test results (a: Pore-water pressure vs shear strain; b: Effective stress path vs Shear stress)

5.3 Hydrodynamic pressure

There is a difference level of seepage water in the process of groundwater infiltrating to the front of the slope due to the rise in groundwater resulting in seepage pressure in the experimental slope. To study the change in seepage pressure of the experimental slope during groundwater rising, a two-dimensional slope with 40° was established using a sigma/W module based on the results of the experiment. The shape and soil parameters of the simulation slope are the same as that of the experimental slope protected by a flat slope in the physical model experiment. The lower boundary of the simulation slope is set as the impermeable boundary (unit flow is zero), the left boundary is set with a constant head of 50 cm, and the other boundary is set as the default boundary, and the simulation process lasted for seven hours.

Figure 12 shows the water pressure distribution at different times. In the early stage of the test, the water pressure of the slope develops in a diffusive way. The soil mass at the place of groundwater infiltration changes first, and the water pressure gradually rises and tends to stabilize. The variation area of water pressure extends from the back edge of the slope to the front edge of the slope. The water pressure of the slope shows obvious stratification in the horizontal direction, and the infiltration of water pressure along the back edge of the slope gradually decreases towards the front of the slope. There is a water pressure gradient from the back of the slope to the front of the slope. The water pressure gradient will increase the probability of slope instability, reduce the stability of the slope, and promote the slope failure.

Figure 12 Water pressure variation of the slope

6. Conclusion

The Gully Stabilization and Highland Protection project was widely developed in the Loess Plateau, which was proven to be an effective means to alleviate gully erosion in the Dongzhiyuan tableland. Note that although the implementation of the Gully Stabilization and Highland Protection could effectively alleviate the gully erosion and soil erosion, the design and implementation of this project should be based upon scientific study of the erosion characteristics of the gully. Loess has special characteristics of macro-pores, vertical joints, loose texture, and water sensitivity, which makes it prone to erosion, especially the remolded loess. The Gully Stabilization and Highland Protection project used remolded loess to fill in the ditch, which led to the increase in groundwater. Otherwise, the implementation of this project would not be able to alleviate the gully erosion; rather, it might lead to various engineering disasters and ecological problems. From the experiments, the processes of a loess-filled slope failure process triggered by groundwater rising were studied and the following conclusions were drawn:

1. With rising groundwater, the groundwater initially infiltrates the filled slope uniformly. Then deformation and cracks appear in the slope due to preferential seepage. In this process, it is accompanied by suffusion erosion, migration of fine particles, structural damage, collapsible settlement, and cracks.

2. The soil at the toe of the slope reaches saturation when the groundwater flows out at the foot of the slope, and then the flow-slip phenomenon occurs first, leading to regressive failure of the fill slope. The failure process of the experimental slope can be divided into three stages: settlement deformation, collapse deformation, and slope toe slide-flow and regressive failure.

3. The groundwater rises and infiltrates into the filled loess slope resulting in suffusion erosion, saturation softening, and hydrodynamic pressure.

Therefore, the filled loess slope should be well drained of groundwater, and the outflow of groundwater should be designed to prevent the groundwater infiltrating into the filled loess slope.

Acknowledgements

The authors are very grateful to the anonymous reviewers and editors for their thoughtful review comments and suggestions which have significantly improved this paper. This study was financially supported by the National Natural Science Foundation of China (NSFC): 41941019, 41790444, 41922054 and Fundamental Research Funds for the Central Universities, CHD 300102260302, 300102260405.

References

Bendahmane F, Marot D, Alexis A. 2008. Experimental parametric study of suffusion and backward erosion. *J. Geotech Geoenviron Eng* **134(1)** : 57–67.

Chang DS, Zhang LM. 2013. Critical hydraulic gradients of internal erosion under complex stress states. *J. Geotech Geoenviron Eng* **139(9)** : 1454–1467.

Chapuis RP. 1992. Similarity of internal stability criteria for granular soils. *Canadian Geotechnical Journal* **29(4)** : 711–713.

Chen SY, Xu JM, Wang WL, Zhao AC, Li HY. 2009. erosion features of head-cut and its control measures on dongzhiyuan of the loess plateau. *Bulletin of Soil and Water Conservation* **29(4)** : 37-41.

Crosta G, di Prisco C. 1999. On slope instability induced by seepage erosion. *Canadian Geotechnical Journal* **36(6)** : 1056–1073.

Derbyshire E, Meng XM, Dijkstra TA. 2000. Landslides in the Thick Loess Terrain of North-West China. J*ohn Wiley & Sons Ltd* London.

Derbyshire E. 2001. Geological hazards in loess terrain, with particular reference to the loess regions of China. *Earth Sci. Rev* .**54** : 231–260.

Dijkstra TA, Rogers CDF, van Asch TWJ. 1995. Cut slope and terrace edge failures in Malan loess, Lanzhou, PR China. *In Proceedings of the XI ECSMFE conference, Copenhagen* 61-67.

Fan XM, Xu Q, Scaringi G, Li S, Peng DL. 2017. A chemo-mechanical insight into the failure mechanism of frequently occurred landslides in the Loess Plateau, Gansu Province, China. *Engineering Geology* **228(13)** :337-345.

Jin Z, Guo L, Wang YQ, Yu YP, Lin H, Chen YP, Chu GC, Zhang J, Zhang NP. 2019. Valley reshaping and damming induce water table rise and soil salinization on the Chinese Loess Plateau. *Geoderma* **339** : 115-125.

Kenney TC, Lau D. 1985. Internal stability of granular filters. *Canadian Geotechnical Journal* **22(2)** :215–225.

Kovacs G. 1981. Seepage Hydraulics. *Elsevier Scientific Publishing Company Amsterdam* Netherlands.

Langevin CD, Guo W. 2010. MODFLOW/MT3DMS–Based Simulation of Variable-Density Ground Water Flow and Transport. *Groundwater* **44(3)** : 339-351.

Li PY, Qian H, Wu JH. 2014. Accelerate research on land creation.*Nature* **510(7503)** : 29-31.

Li Z, Lin X, Coles AE, Chen X. 2017. Catchment-scale surface water-groundwater connectivity on China Loess Plateau. *Catena***152** : 268-276.

Liu TS. 1985. Loess and the Environment. *Science Press* Beijing.

Lu H, Mason JA, Stevens T, Zhou Y, Yi S, Miao X. 2011. Response of surface processes to climatic change in the dunefields and Loess Plateau of North China during the late Quaternary. *Earth Surface Processes and Landforms***36(12)** : 1590-1603.

Mao CX. 2005. Study on piping and filters: part 1 of piping. *Rock and Soil Mechanics* **26 (2)** : 209–215.

Moffat R, Fannin RJ, Garner SJ. 2011. Spatial and temporal progression of internal erosion in cohesionless soil. *Canadian Geotechnical Journal* **48(3)** :399–412.

Moffat RA, Fannin RJ. 2006. A large permeameter for study of internal stability in cohesionless soils.*Geotech Test J* **29(4)** : 273–279.

Peng JB, Zhuang JQ, Wang GH, Dai FC, Zhang FY, Huang WL, Xu Q. 2018. Liquefaction of loess landslides as a consequence of irrigation.*Quarterly Journal of Engineering Geology and Hydrogeology***51(3)** : 330-337.

Qi X, Xu Q, Liu FZ. 2017. Analysis of retrogressive loess flowslides in Heifangtai, China.*Engineering Geology* **236** : 119–128.

Richards KS, Reddy KR. 2007. Critical appraisal of piping phenomena in earth dams. *Bulletin of Engineering Geology and the Environment***66** : 381–402.

Sassa K. 1985. The mechanism of debris flows. *In Proc., XI Int'l. Conf Soil Mech. Found. Engrg., San Francisco* **3** : 1173-1176.

Scholte's L, Hicher PY, Sibille L. 2010. Multiscale approaches to describe mechanical responses induced by particle removal in granular materials. *Comptes Rendus Mecanique* **338(10)** : 627–638.

Shi XG, Xu Q, Zhang L, Zhao KY, Dong J, Jiang HJ, Liao MS. 2019. Surface displacements of the Heifangtai terrace in Northwest China measured by X and C-band InSAR observations. *Engineering Geology***259** :105181.

Shi YH. 1987. Evolution of gullies on the Loess Plateau in historical period. *Journal of Chinese Historical Geography* **2** :3-54.

Singh A, Krause P, Panda SN, Flugel W.A. 2010. Rising water table: a threat to sustainable agriculture in an irrigated semi-arid region of Haryana, India. Agric.*Water Management* **97** : 1443–1451.

Song YX, Peng JB, Zhang J. 2008. Deformation mechanism of high loess embankment slope. *Journal of Engineering Geology* **16(5)** : 620-624.

Vallejo LE. 2001. Interpretation of the limits in shear strength in binary granular mixtures. *Canadian Geotechnical Journal***38** :1097–1104.

Wang JD, Xu YJ, Yan M, Qiao SN, Feng KQ. 2018. Study on the deformation and failure modes of filling slope in loess filling engineering: a case study at a loess mountain airport. *Landslides* **15** : 2423–2435.

Wu Y, Cheng H. 2005. Monitoring of gully erosion on the loess plateau of china using a global positioning system. *Catena* **63(2-3)** : 154-166.

Xifeng Soil and water conservation Observation station of Yellow River Conservancy Commission of the Ministry of Water Resources. 2005. Research on Soil and Water Loss on the Loess Plateau and Its Comprehensive Control. *Yellow River Conservancy Press Zhengzhou* .

Yang YH,, Wang LQ, Su ZC, Chai ZC. 2003. The Study about Intensity Characteristic and Influence Factors of Remolded Loess. *Journal of Lanzhou Railway University (Natural Sciences)* **22(3)** : 38-412.

Yin X, Chen L, He J, Feng X, Zeng W. 2016. Characteristics of groundwater flow field after land creation engineering in the hilly and gully area of the loess plateau. *Arabian Journal of Geoences***9(14)** : 646.

Yin X, Chen L, He J, Feng X, Zeng W. 2016. Characteristics of groundwater flow field after land creation engineering in the hilly and gully area of the loess plateau. *Arabian Journal of Geoences***9(14)** : 646.

Yin YP, Li B, Wang WP, Zhan LT, Xu Q, Gao Y, Zhang N, Chen HQ, Liu TK, Li AG. 2016. Mechanism of the December 2015 Catastrophic Landslide at the Shenzhen Landfill and Controlling Geotechnical Risks of Urbanization[J]. *Engineering* **2(2)** :230-249.

Yu DF, He QL, Du H, Fan DG, Wang K, Liu KH. 2014. The Application of Geophysical Methods to Finding out Water Content Characteristics in Heifangtai Watering Aarea. *Chinese Journal of Engineering Geophysics* **11(3)** : 422-425.

Zhang D, Wang G, Luo C, Chen J, Zhou Y. 2009. A rapid loess flowslide triggered by irrigation in China. Landslides **6(1)** : 55–60.

Zhang FY, Wang GH. 2018. Effect of irrigation-induced densification on the post-failure behavior of loess flowslides occurring on the Heifangtai area, Gansu, China. *Engineering Geology***236(11)** :111-118.

Zhang FY,, Yan BB, Feng XM, Lan HX, Kang C, Lin XS, Zhu XH, MA WG. 2019. A rapid loess mudflow triggered by the check dam failure in a bulldoze mountain area, Lanzhou, China. *Landslides* **16** : 1981-1992.

Zhang XL, Xu Q, Peng DL, Zhao KY, Liu L, Ren J. 2017. Application of high-density resistivity method to groundwater exploration in Heifangtai. *Progress in Geophysics (in Chinese)* **32(4)** : 1862-1867.

Zhao JJ, Yu JL, Xie ML, Chai HJ, Li T, Bu F, Lin B. 2018. Physical model studies on fill embankment slope deformation mechanism under rainfall condition.*Rock and Soil Mechanics* **39(8)** :2933-2940.

Zhuang J, Peng J, Wang G, Iqbal J, Wang Y, Li W, Xu Q, Zhu X. 2017. Prediction of rainfall-induced shallow landslides in the Loess Plateau, Yan'an, China, using the TRIGRS model. *Earth Surface Processes and Landforms* **42(6)** : 915-927.

Zhuang JQ, Cui P, Hu KH, Chen XQ. (2015b) Fine particle size moving and it's effective on debris flow initiation.*J Mountain Research* **33(6)** :713-720.

Zhuang JQ, Peng JB, Iqbal J, Liu TM, Liu N, Li YZ, Ma PH. 2015a. Identification of landslide spatial distribution and susceptibility assessment in relation to topography in the Xi'an region, Shaanxi province, China. *Frontiers of Earth Science***9(3)** :449-462.

Zhuang JQ, Peng JB. 2014. A coupled slope cutting-a prolonged rainfall-induced loess landslide: a 17 October 2011 case study. *Bulletin of Engineering Geology and the Environment* **73(4)** : 997-1011.

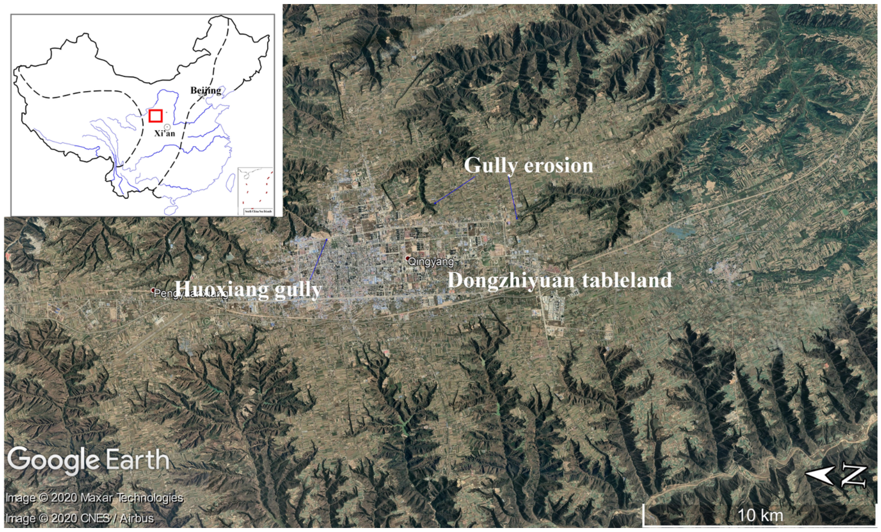
Beijing
Xi'an
Gully erosion
Qingyang
Huoxiang gully
Dongzhiyuan tableland
Google Earth
Image © 2020 Maxar Technologies
Image © 2020 CNES / Airbus
10 km


Erosion
2m
Erosion
2m
Collapse
Erosion
4m
Collapse
4m
2m

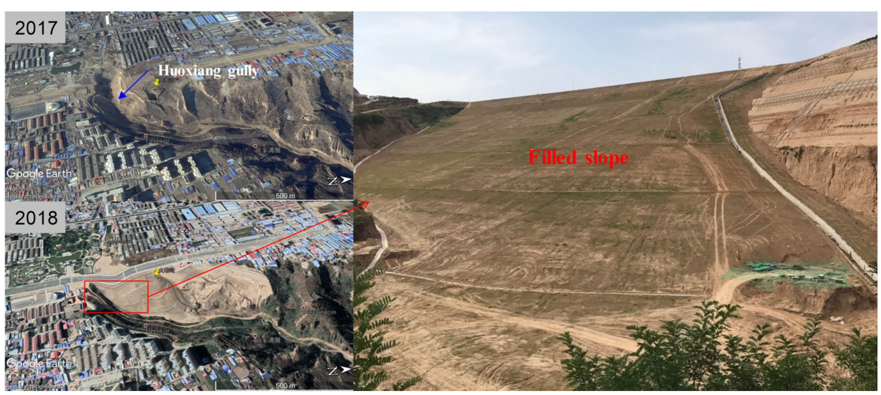
2017
Huoxiang gully
Google Earth
2018
Filled slope

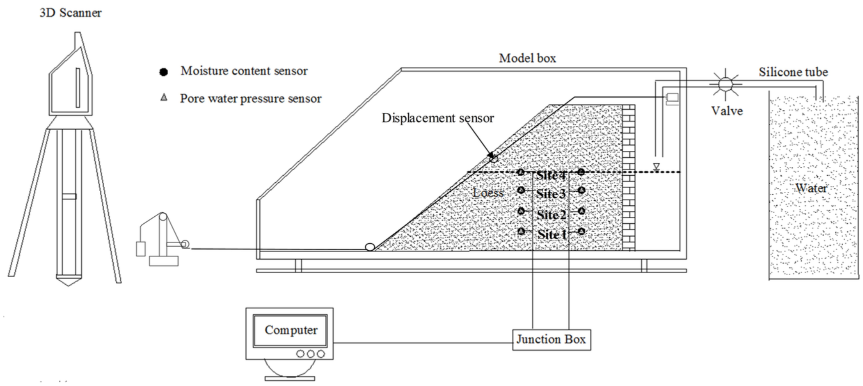
3D Scanner
Moisture content sensor
Pore water pressure sensor
Model box
Silicone tube
Valve
Displacement sensor
Loess
Site4
Site3
Site2
Site1
Water
Computer
Junction Box

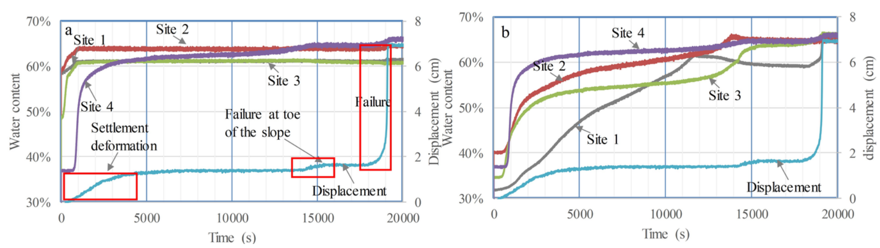
a
Site 1
Site 2
Site 3
Site 4
Settlement deformation
Failure at toe of the slope
Failure
Displacement
Water content
Displacement (cm)
Time (s)
b
Site 4
Site 2
Site 3
Site 1
Displacement
Water content
displacement (cm)
Time (s)

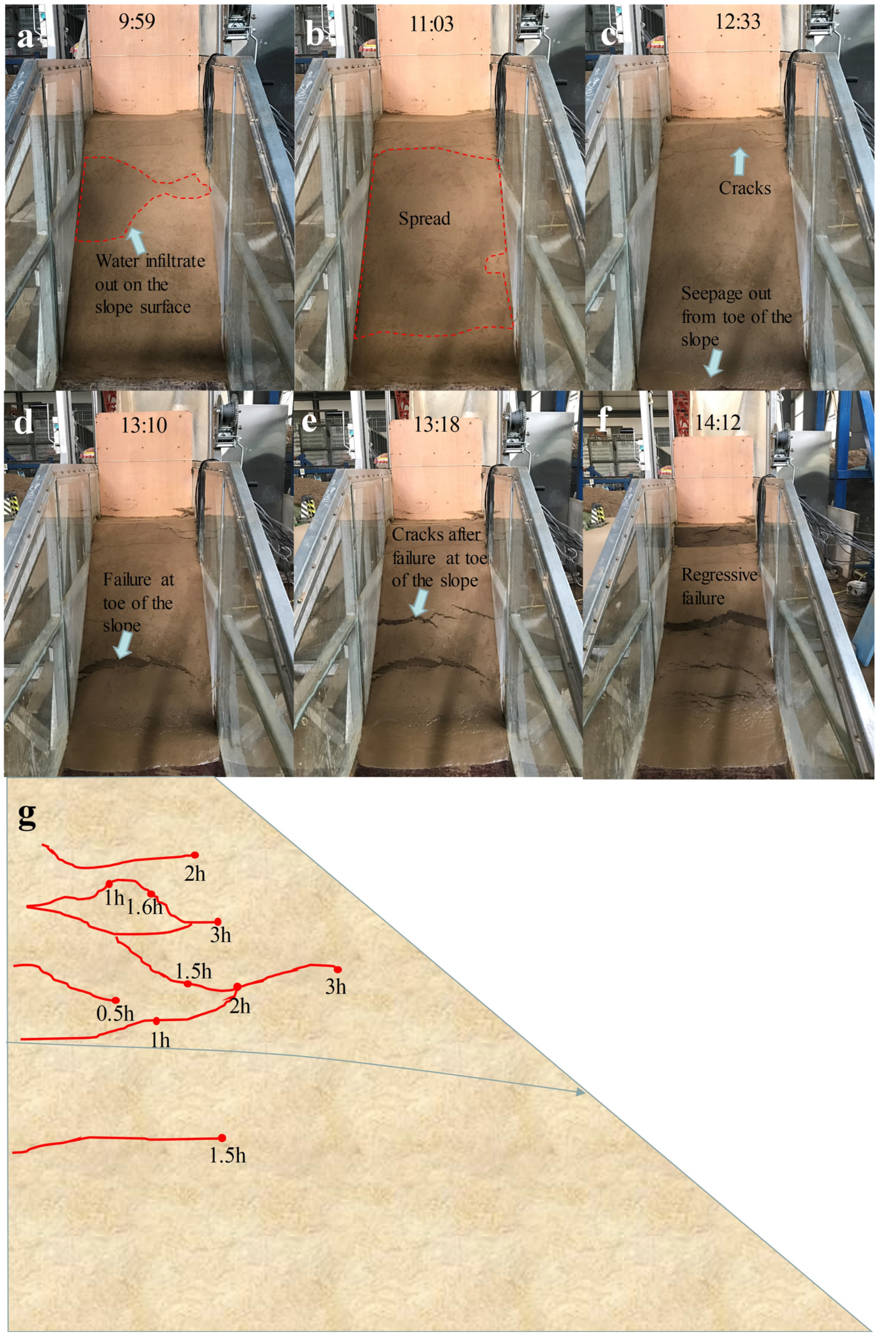
a
9:59
Water infiltrate out on the slope surface
b
11:03
Spread
c
12:33
Cracks
Seepage out from toe of the slope
d
13:10
Failure at toe of the slope
e
13:18
Cracks after failure at toe of the slope
f
14:12
Regressive failure
g
2h
1h
1.6h
3h
1.5h
3h
0.5h
2h
1h
1.5h

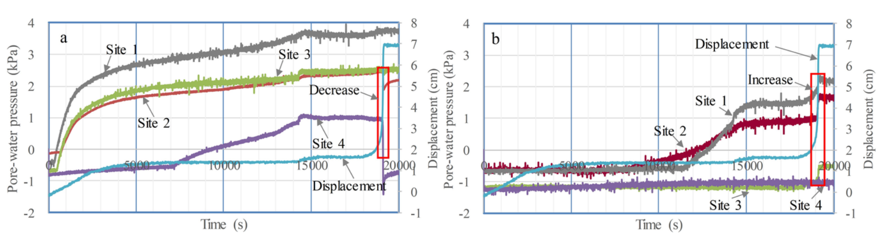
a
Site 1
Site 3
Site 2
Decrease
Site 4
Displacement
Pore-water pressure (kPa)
Displacement (cm)
Time (s)
b
Displacement
Increase
Site 1
Site 2
Site 3
Site 4
Pore-water pressure (kPa)
Displacement (cm)
Time (s)

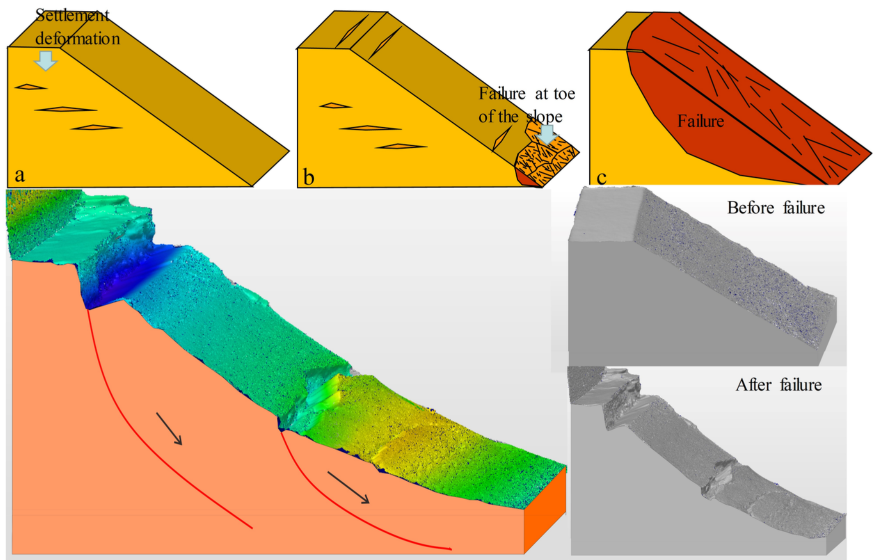
Settlement deformation
a
Failure at toe of the slope
b
Failure
c
Before failure
After failure

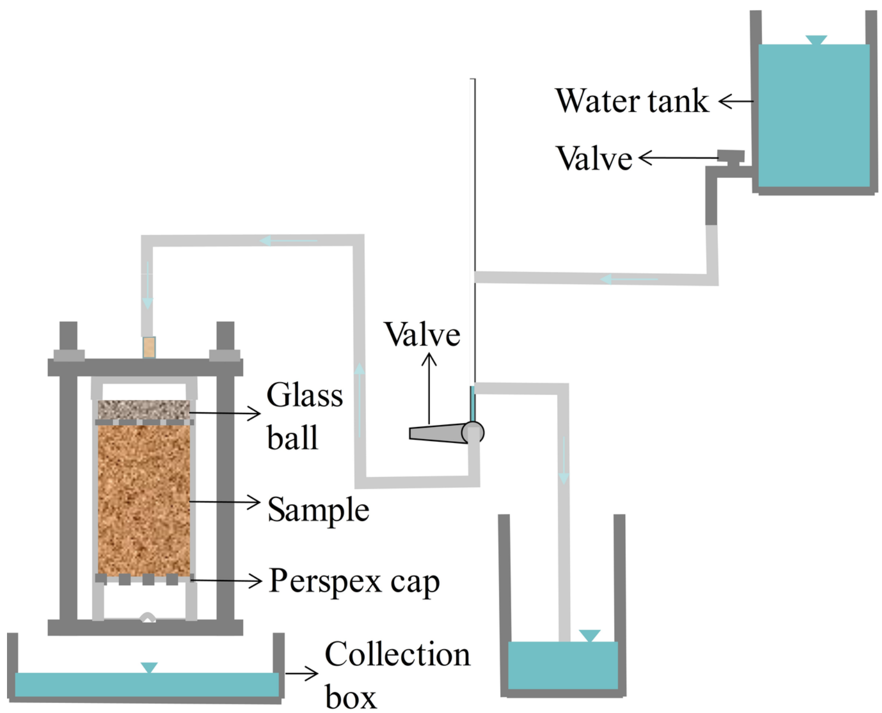
Water tank
Valve
Valve
Glass ball
Sample
Perspex cap
Collection box

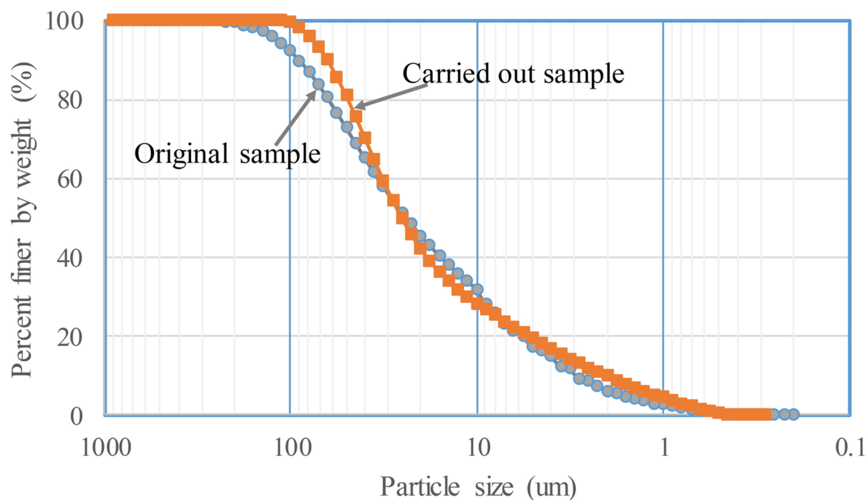
Carried out sample
Original sample
Percent finer by weight (%)
Particle size (um)
100
80
60
40
20
0
1000
100
10
1
0.1

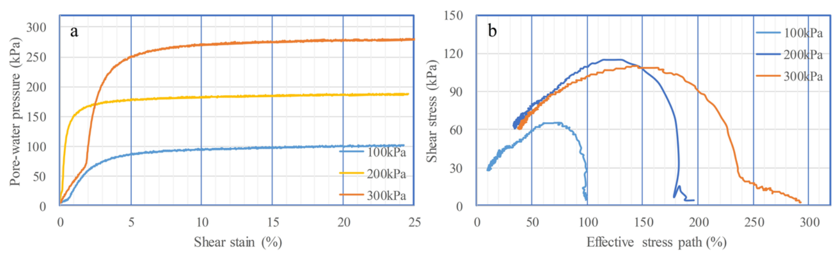
a
Pore-water pressure (kPa)
Shear stain (%)
100kPa
200kPa
300kPa
b
Shear stress (kPa)
Effective stress path (%)
100kPa
200kPa
300kPa

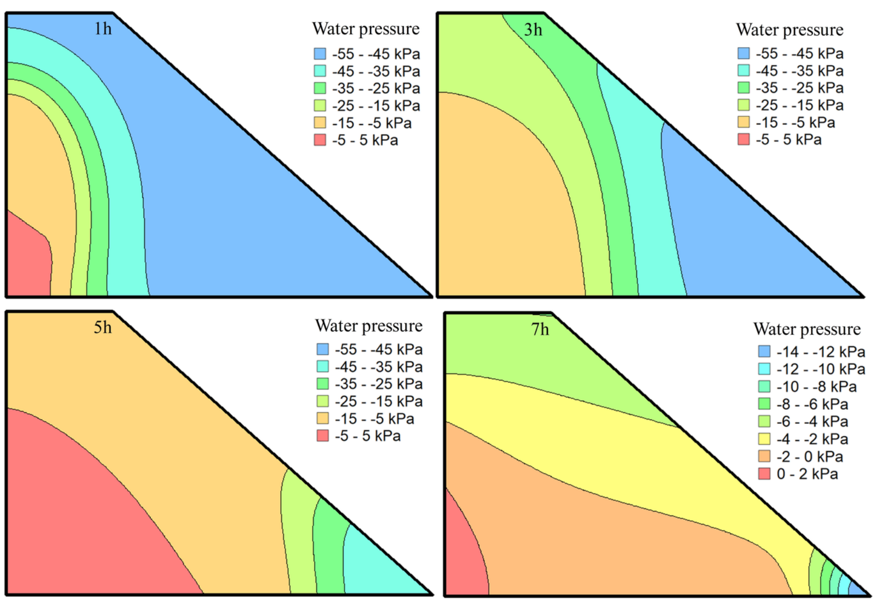
1h
Water pressure
-55 - -45 kPa
-45 - -35 kPa
-35 - -25 kPa
-25 - -15 kPa
-15 - -5 kPa
-5 - 5 kPa
3h
Water pressure
-55 - -45 kPa
-45 - -35 kPa
-35 - -25 kPa
-25 - -15 kPa
-15 - -5 kPa
-5 - 5 kPa
5h
Water pressure
-55 - -45 kPa
-45 - -35 kPa
-35 - -25 kPa
-25 - -15 kPa
-15 - -5 kPa
-5 - 5 kPa
7h
Water pressure
-14 - -12 kPa
-12 - -10 kPa
-10 - -8 kPa
-8 - -6 kPa
-6 - -4 kPa
-4 - -2 kPa
-2 - 0 kPa
0 - 2 kPa